


# Improving the spectral purity of single photons by a single-interferometer-coupled microring

Yang Wang(王洋), Pingyu Zhu(朱枰谕), Shichuan Xue(薛诗川), Yingwen Liu(刘英文),Junjie Wu(吴俊杰), Xuejun Yang(杨学军), and Ping Xu(徐平)

**Citation:**Chin. Phys. B, 2022, 31 (**3**): 034210. DOI: 10.1088/1674-1056/ac3652
Journal homepage: http://cpb.iphy.ac.cn; http://iopscience.iop.org/cpb

**What follows is a list of articles you may be interested in**

---

## High-performance and fabrication friendly polarization demultiplexer

Huan Guan(关欢), Yang Liu(刘阳), and Zhiyong Li (李智勇)
Chin. Phys. B, 2022, 31 (**3**): 034203. DOI: 10.1088/1674-1056/ac21bc

## Bright 547-dimensional Hilbert-space entangled resource in 28-pair modes biphoton frequency comb from a reconfigurable silicon microring resonator

Qilin Zheng(郑骑林), Jiacheng Liu(刘嘉成), Chao Wu(吴超), Shichuan Xue(薛诗川), Pingyu Zhu(朱枰谕), Yang Wang(王洋), Xinyao Yu(于馨瑶), Miaomiao Yu(余苗苗), Mingtang Deng(邓明堂), Junjie Wu(吴俊杰), and Ping Xu(徐平)
Chin. Phys. B, 2022, 31 (**2**): 024206. DOI: 10.1088/1674-1056/ac3507

## Bandwidth-tunable silicon nitride microring resonators

Jiacheng Liu(刘嘉成), Chao Wu(吴超), Gongyu Xia(夏功榆), Qilin Zheng(郑骑林), Zhihong Zhu(朱志宏), and Ping Xu(徐平)
Chin. Phys. B, 2022, 31 (**1**): 014201. DOI: 10.1088/1674-1056/ac2e64

## Near 100% spectral-purity photons from reconfigurable micro-rings

Pingyu Zhu(朱枰谕), Yingwen Liu(刘英文), Chao Wu(吴超), Shichuan Xue(薛诗川), Xinyao Yu(于馨瑶), Qilin Zheng(郑骑林), Yang Wang(王洋), Xiaogang Qiang(强晓刚), Junjie Wu(吴俊杰), and Ping Xu(徐平)
Chin. Phys. B, 2020, 29 (**11**): 114201. DOI: 10.1088/1674-1056/abbb28

## Characterize and optimize the four-wave mixing in dual-interferometer coupled silicon microrings

Chao Wu(吴超), Yingwen Liu(刘英文), Xiaowen Gu(顾晓文), Shichuan Xue(薛诗川), Xinxin Yu(郁鑫鑫), Yuechan Kong(孔月婵), Xiaogang Qiang(强晓刚), Junjie Wu(吴俊杰), Zhihong Zhu(朱志宏), Ping Xu(徐平)
Chin. Phys. B, 2019, 28 (**10**): 104211. DOI: 10.1088/1674-1056/ab3f9b

---

# Improving the spectral purity of single photons by a single-interferometer-coupled microring

Yang Wang(王洋), Pingyu Zhu(朱枰谕), Shichuan Xue(薛诗川), Yingwen Liu(刘英文), Junjie Wu(吴俊杰), Xuejun Yang(杨学军), and Ping Xu(徐平)†

*Institute for Quantum Information & State Key Laboratory of High Performance Computing, College of Computer Science and Technology, National University of Defense Technology, Changsha* 410073, *China*

(Received 22 September 2021; revised manuscript received 1 November 2021; accepted manuscript online 4 November 2021)

We experimentally engineer a high-spectral-purity single-photon source using a single-interferometer-coupled silicon microring. By the reconfiguration of the interferometer, different coupling conditions can be obtained, corresponding to different quality factors for the pump and signal/idler. The ratio between the quality factor of the pump and signal/idler ranges from 0.29 to 2.57. By constructing the signal–idler joint spectral intensity, we intuitively demonstrate the spectral correlation of the signal and idler. As the ratio between the quality factor of the pump and signal/idler increases, the spectral correlation of the signal and idler decreases, i.e., the spectral purity of the signal/idler photons increases. Furthermore, time-integrated second-order correlation of the signal photons is measured, giving a value up to $94.95 \pm 3.46\%$. Such high-spectral-purity photons will improve the visibility of quantum interference and facilitate the development of on-chip quantum information processing.

**Keywords:** spectral-purity, microring, asymmetric Mach–Zehnder interferometer

**PACS:** 42.82.−m, 42.82.Et, 42.65.−k, 42.65.Wi **DOI:** 10.1088/1674-1056/ac3652

## 1. Introduction

High-quality and deterministic single-photon sources play a critical role in quantum information processing, including quantum cryptography[1,2] and linear-optical quantum computation.[3,4] Single-emitter-based single-photon sources and heralded single-photon sources via spontaneous parametric process are two typical approaches to generate on-demand single photons. The former has been realized on different quantum systems such as quantum dots,[5,6] single atom[7,8] and color centers.[9] A typical implementation of the latter is via spontaneous four-wave mixing (SFWM) in integrated quantum photonic circuits (IQPCs). The heralded single-photon source based on SFWM in IQPCs holds the advantage of scalability, robustness, energy efficiency and compactness.

Quantum light sources based on SFWM have been implemented on a variety of platforms, such as silicon-on-insulator (SOI),[10] silica-on-silicon,[11] and SiN-on-silica.[12] Of all these platforms, SOI is especially appealing for its CMOS-compatibility and holds great potential in fully integrated photonic chips toward high-performance quantum information processing. Due to the high refractive index contrast,[13] large third-order nonlinear coefficient[14] and compact volume, silicon microrings have dramatically increased SFWM efficiency under a relatively low pump power.[15] The bright photon-pair source has been implemented using a dual-interferometer-coupled silicon microring.[16] Apart from the brightness, the spectral purity of single photons is another essential property to ensure high-visibility quantum interference. The converted photon pairs should be unentangled in frequency to ensure the heralded single photons in the spectrally pure state. Using a narrowband filter to post-select the converted photons is a simple way to obtain high spectral purity, with the sacrifice of single photon counts and the heralding efficiency. Another approach for pursuing high-spectral-purity single-photon source has been proposed theoretically[17] and demonstrated experimentally.[18] Fully separable biphoton wavefunction is engineered using dual-interferometer-coupled microring, which does not sacrifice the heralding efficiency. The high spectral purity from dual-interferometer-coupled microring benefits from independently tuning quality factors of the pump and converted photons, compared with the one or double straight-waveguide coupled microring whose upper bound on spectral purity is 93%.[20,21] However, a series of dual-interferometer-coupled microrings with different coupling parameters need to be fabricated to confirm the optimal one since the quality factors are fixed after the manufacture of the chip.

In this work, we use a single-interferometer-coupled microring to achieve and characterize high-spectral-purity single-photon source. The microring coupled by an asymmetric Mach–Zehnder interferometer (AMZI) can be configured to get different quality factors for the pump and converted photons. We experimentally engineer the spectral purity of the heralded photons over 93% following the method in Ref. [19]. It is a fabrication-friendly scheme to generate high-spectral-purity single photons because of its reconfigurability. This spectral-purity-reconfigurable single-photon source is desired

†Corresponding author. E-mail: pingxu520@nju.edu.cn

© 2022 Chinese Physical Society and IOP Publishing Ltd 

in multiphoton interference research, such as disclosing the relationship of fidelity and distinguishability of photons in Boson sampling.[22]

## 2. Theory

The normalized two-photon state from SFWM can be represented as

$$|\psi\rangle = \iint \mathrm{d}\omega_\mathrm{s}\mathrm{d}\omega_\mathrm{i}\phi(\omega_\mathrm{s},\omega_\mathrm{i})\, a^\dagger_{\omega_\mathrm{s}} a^\dagger_{\omega_\mathrm{i}} |0\rangle, \tag{1}$$

where $a^\dagger_{\omega_\mathrm{s}}$ ($a^\dagger_{\omega_\mathrm{i}}$) is the creation operator of the signal (idler) photons with angular frequency $\omega_\mathrm{s}$ ($\omega_\mathrm{i}$).[17] $\phi(\omega_\mathrm{s},\omega_\mathrm{i})$ is the joint spectral function in the form

$$\begin{aligned}\phi(\omega_\mathrm{s},\omega_\mathrm{i}) = &\int \mathrm{d}\omega_\mathrm{p}\alpha(\omega_\mathrm{p})\,\alpha(\omega_\mathrm{s}+\omega_\mathrm{i}-\omega_\mathrm{p}) \\ &\times l(\omega_\mathrm{p})\, l(\omega_\mathrm{s}+\omega_\mathrm{i}-\omega_\mathrm{p})\, l(\omega_\mathrm{s})\, l(\omega_\mathrm{i}).\end{aligned} \tag{2}$$

The normalized pump laser's spectral distribution $\alpha(\omega_\mathrm{p})$ is usually in Gaussian mode, and the resonances of pump, signal and idler are described by Lorentzian function

$$l(\omega) = \mathrm{i}\kappa / \left(1 - t\cdot \mathrm{e}^{\mathrm{i}\beta(\omega)L}\cdot \mathrm{e}^{-\eta L}\right), \tag{3}$$

where $\kappa$ and $t$ are respectively the cross-coupling and self-coupling coefficients between the bus waveguide and microring, $\beta(\omega)$ is the propagation constant for angular frequency $\omega$, $L$ is the roundtrip length of the microring, and $\eta$ is the effective loss coefficient of the microring.

The detection of one photon in the converted photon pair heralds the existence of the other. If the joint spectral function is narrowly peaked at $\Omega_\mathrm{s}+\Omega_\mathrm{i} = 2\Omega_\mathrm{p}$, where $\Omega_\mathrm{s}$, $\Omega_\mathrm{i}$ and $\Omega_\mathrm{p}$ are the central frequencies of the signal, idler and pump, the converted photon pair will be highly anti-correlated in frequency. In this situation, the heralded single photon is in a mixed state. The strict correlation can be relaxed by broadening the pump spectrum, giving rise to spectrally pure single photons. Except for a sufficiently spectrally broad pump laser, the pump resonance linewidth must be much broader than the signal's and idler's to get high spectral purity of the heralded photons. The full width at half-maximum of the resonance at frequency $\omega$ is $\omega/Q$, where $Q$ stands for the quality factor of the microring. Therefore, to achieve high spectral purity of single photons the pump quality factor $Q_\mathrm{p}$ must be significantly smaller than signal quality factor $Q_\mathrm{s}$ and idler quality factor $Q_\mathrm{i}$. The purity of the heralded single photon can be calculated by $p = 1/K$, where $K = X^2/Y$ is the Schmidt number[23] and $X = \int \mathrm{d}\omega_\mathrm{s}\int \mathrm{d}\omega_\mathrm{i}\,|\phi(\omega_\mathrm{s},\omega_\mathrm{i})|^2$, $Y = \int \mathrm{d}\omega_\mathrm{s}\int \mathrm{d}\omega_\mathrm{i}\int \mathrm{d}\omega_\mathrm{s}'\int \mathrm{d}\omega_\mathrm{i}'[\phi(\omega_\mathrm{s},\omega_\mathrm{i})\phi(\omega_\mathrm{s}',\omega_\mathrm{i}')\phi^*(\omega_\mathrm{s},\omega_\mathrm{i}')\phi^*(\omega_\mathrm{s}',\omega_\mathrm{i})]$. Assuming the injected pump laser's spectrum is sufficiently broad, we numerically calculate the spectral purity as a function of $Q_\mathrm{s/i}/Q_\mathrm{p}$. As shown in Fig. 1, higher purity is expected by increasing the ratio $Q_\mathrm{s/i}/Q_\mathrm{p}$.

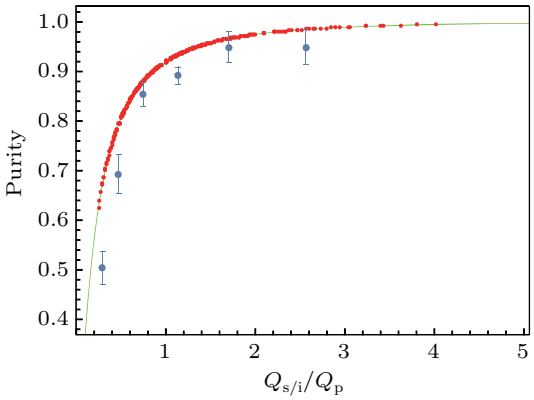



**Fig. 1.** Spectral purity as a function of $Q_\mathrm{s/i}/Q_\mathrm{p}$. The red dots are samples generated using parameters corresponding to our chip; the green line is spectral purity function of $Q_\mathrm{s/i}/Q_\mathrm{p}$ fitted from the simulated samples; and the blue dots with error bars are purities detected experimentally.

The total quality factor contains intrinsic and extrinsic quality factor

$$\frac{1}{Q_\mathrm{p}} = \frac{1}{Q_\mathrm{int}} + \frac{1}{Q_\mathrm{ext,p}}, \quad \frac{1}{Q_\mathrm{s/i}} = \frac{1}{Q_\mathrm{int}} + \frac{1}{Q_\mathrm{ext,s/i}}. \tag{4}$$

The roundtrip loss of the ring determines the intrinsic quality factor $Q_\mathrm{int}$, while the effective coupling coefficient of the interferometric coupler determines the extrinsic quality factor $Q_\mathrm{ext}$,

$$Q_\mathrm{ext} = \frac{\omega L}{v_\mathrm{g}\,|\kappa_\mathrm{eff}|^2}. \tag{5}$$

An AMZI-coupled microring structure is used to manipulate the coupling conditions of the pump and signal/idler to optimize the spectral purity of the generated photons, as shown in Fig. 2. Assuming the intrinsic quality factors are constant, the quality factors of the pump and signal/idler are determined by the effective coupling coefficient. The path difference of AMZI is half of the ring's roundtrip, $\pi R$, in the original proposal in Ref. [19]. To avoid the heat crosstalk between heaters in AMZI and microring, the path difference of AMZI is set to $3\pi R$ in our experiment. The effective coupling coefficient configured by the AMZI satisfies

$$\left|\kappa_{\mathrm{eff,\ p(s/i)}}\right|^2 = 2\kappa^2(1-\kappa^2)\left[1+\cos(\beta_\mathrm{p(s/i)}\Delta l+\theta)\right], \tag{6}$$

where $\beta_\mathrm{p(s/i)}$ is the propagation constant of the pump (signal/idler) and $\Delta l$ is the length difference between the long and short arms of the AMZI. The AMZI with $3\pi R$ path difference gives $3\pi$ phase shift between adjacent resonances assigned as the pump and signal/idler, i.e., if the pump is set to be maximally coupled into (out from) the microring, the signal and idler resonance will be suppressed. Suppose $\varphi = \beta_\mathrm{p}\Delta l + \theta$ and the constant $A = Q_\mathrm{int}/Q_{\mathrm{ext},\varphi=0}$ is the ratio of the intrinsic and maximal extrinsic quality factor. We can control the extrinsic quality factor by the phase-shifter in the AMZI following

$$\frac{Q_\mathrm{s/i}}{Q_\mathrm{p}} = \frac{\dfrac{1}{Q_\mathrm{int}}+\dfrac{1}{Q_\mathrm{ext,p}}}{\dfrac{1}{Q_\mathrm{int}}+\dfrac{1}{Q_\mathrm{ext,s/i}}} = \frac{2+A(1+\cos\varphi)}{2+A\left[1+\cos(\varphi+3\pi)\right]}. \tag{7}$$

The ratio of $Q_{s/i}$ and $Q_p$ can be set in the range of $(1/(1+A),\ 1+A)$, so we can get different purities of single photons.

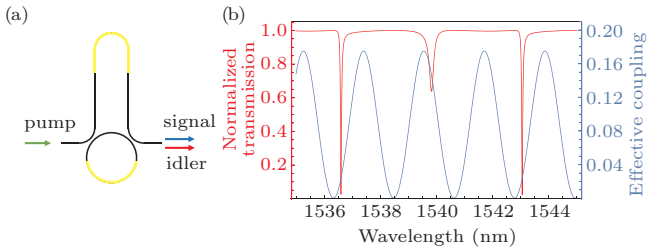



**Fig. 2.** (a) Schematic of AMZI-coupled microring. (b) The transmission spectra of the AMZI-coupled microring and the corresponding effective coupling.

## 3. Experiment

Experimentally, we fabricate an AMZI-coupled microring on an SOI chip. The height of the silicon waveguide in silica is 220 nm, and the width is 450 nm. The roundtrip length of the microring is $2\pi \cdot 28$ μm. Free spectral range (FSR) of 3.2 nm is implemented to align the standard dense wavelength division multiplexing (DWDM) channels. The gaps at the two coupling points of the AMZI are both 180 nm. Thermo-optic modulators on the long arm of AMZI and microring are respectively used to tune the interferometer phase and resonant wavelength. The experiment setup is shown in Fig. 3. The pulsed laser with a repetition frequency of 60 MHz is used as the pump laser, which is filtered by a 200 GHz DWDM to suppress sideband noise. A continuous-wave (CW) laser is introduced as the seed signal for joint spectral correlation measurement. The two lasers are combined by a 50:50 fiber beam splitter. The grating couplers couple in and out the pump, seed and converted photons through an off-chip fiber array.

By adjusting the voltage on the phase shifter in AMZI, different effective coupling coefficients are configured. To get the transmission spectra, we scan the tunable CW laser and record the resonator's transmission power by a power meter. Figure 3 gives the transmission spectra at different voltage configurations. The corresponding quality factors are listed in Table 1. It is hard to maintain exactly equal quality factors of signal and idler, so we take the minimum of $Q_s$ and $Q_i$ to calculate $Q_{s/i}/Q_p$. The ratios $Q_{s/i}/Q_p$ are measured to be 0.29, 0.48, 0.75, 1.14, 1.70 and 2.57. According to the fitting curve in Fig. 1, the purity of the converted photons is expected to be 67.33%, 79.38%, 88.08%, 93.43%, 96.65% and 98.49%, respectively.

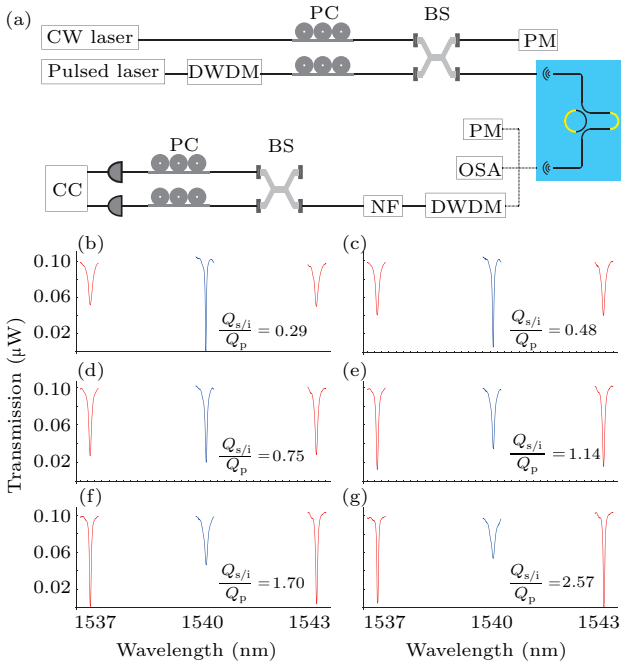



**Fig. 3.** (a) Experimental setup. PC, polarization controller; BS, beam splitter; PM, power meter; OSA, optical spectrum analyzer; CC, coincidence counting module; NF, narrowband filter. (b)–(g) The measured transmission spectrums and the corresponding $Q_{s/i}/Q_p$.

**Table 1.** Summary of main metrics of the AMZI-coupled microring single-photon sources.

| AMZI (V) | $Q_p$ ($10^3$) | $Q_i$ ($10^3$) | $Q_s$ ($10^3$) | $Q_{s/i}/Q_p$ | $P_{theo}$ (%) | $P_{JSI}$ (%) | $P_{g^{(2)}}$ (%) |
|---|---|---|---|---|---|---|---|
| $\sqrt{3}$ | 41.92 | 12.36 | 13.66 | 0.29 | 67.33 | 63.60 | $50.31 \pm 3.34$ |
| $\sqrt{4}$ | 31.45 | 14.95 | 15.56 | 0.48 | 79.38 | 79.03 | $69.31 \pm 3.90$ |
| $\sqrt{5}$ | 23.71 | 17.92 | 17.74 | 0.75 | 88.08 | 75.28 | $85.45 \pm 2.41$ |
| $\sqrt{6}$ | 18.25 | 22.19 | 20.73 | 1.14 | 93.43 | 87.98 | $89.11 \pm 1.79$ |
| $\sqrt{7}$ | 14.68 | 26.26 | 25.00 | 1.70 | 96.65 | 89.70 | $94.91 \pm 3.14$ |
| $\sqrt{8}$ | 11.54 | 29.93 | 29.61 | 2.57 | 98.49 | 94.77 | $94.95 \pm 3.46$ |

By constructing the signal-idler joint spectral intensity (JSI) profile using the stimulated emission tomography (SET) method,[24] we then study the detailed spectral correlation of signal and idler. Figure 4 gives the theoretical and measured JSI profiles. It depicts that the measured JSI profiles agree well with the theoretical ones. A clear frequency anti-correlation is observed when $Q_{s/i}/Q_p < 1$. With the ratio $Q_{s/i}/Q_p$ increasing, the spectral correlation of signal and idler decreases. The SET measurement gives a vivid image of spectral correlation, and supplies the corresponding purity of 63.60%, 79.03%, 75.28%, 87.98%, 89.70% and 94.77%, respectively. Furthermore, both theoretical and experimentally measured JSI profiles suffer from the deformation compared to those in previous work. This is mainly caused by the drastic change of the effective coupling coefficients around the frequency of resonances. In one FSR of 3.2 nm, the effective coupling coefficient of AMZI with $3\pi R$ path difference goes through 1.5 periods, while the effective coupling coefficient of AMZI with $\pi R$ path difference goes through 0.5 periods. The unsymmetry of transmission spectra caused by the drastic change of the effective coupling coefficients can be observed in Fig. 2(b) and experimentally demonstrated in Figs. 3(b)–3(g).

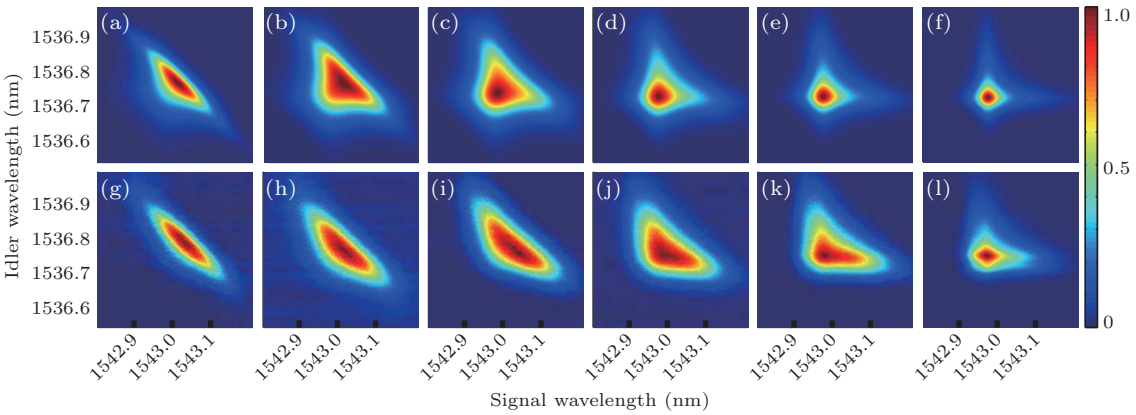



**Fig. 4.** (a)–(f) Theoretical and (g)–(l) experimentally measured signal–idler joint spectral intensity profiles for the ratios $Q_{s/i}/Q_p$ being 0.29, 0.48, 0.75, 1.14, 1.70 and 2.57.

Time-integrated second-order correlation ($g^{(2)}$) is a rigid purity measurement quantitatively describing the number of temporal modes contained in the converted single photons. To measure $g^{(2)}$ of the signal photons, a 100 GHz DWDM is first used to separate signal photons from idlers and transmitted pump. To further suppress the pump noise and photons from the broadband SFWM in the fiber and straight silicon waveguide, a linewidth-tunable narrowband filter (NF) follows the DWDM channel. In order not to post-select the signal's spectrum, the NF linewidth is set to 0.2 nm for signal with quality factor of 13660, 15560, 17740, while the NF linewidth is set to 0.1 nm for signal with quality factor of 20730, 25000, 29610. The signal is then split by a 50:50 fiber beam splitter and detected by two superconducting nanowire single-photon detectors with dark count rates of 29 Hz and 34 Hz, respectively. Single counts and two-fold coincidence count are recorded to calculate $g^{(2)}$, which are listed in Table 1. The $g^{(2)}$ of the signal photons increase with the ratio $Q_{s/i}/Q_p$, and they are marked in Fig. 1. There are three key factors resulting in the measured single photon purity below the theoretical calculation. First, the waveguide connecting the grating coupler and the input port of the microring is 1188 μm, and the waveguide connecting the output port of the microring and the grating coupler is 372 μm. The SFWM in these waveguides also generates photon pairs but with a different joint spectrum which will affect the purity of the detected single photons. Second, there is still transmitted pump power not filtered out by the DWDM and NF, affecting the $g^{(2)}$ measurement of the signal photons. Third, the imperfection of the nano fabrication causes the deformation of the transmission spectra. When the microring works in undercoupling condition, mode-splitting can be observed, indicating that the resonances in the experiment are not perfectly consistent with the theoretical calculation. With the effect of all these factors, the highest purity of $94.95 \pm 3.46\%$ is implemented in our AMZI-coupled silicon microring.

## 4. Conclusion

We have experimentally demonstrated and characterized a spectral-purity-reconfigurable single-photon source based on an AMZI-coupled silicon microring. The JSI profiles intuitively demonstrate the decrease of correlation between signal and idler as the ratio of signal/idler and pump quality factor increases. The single photon $g^{(2)}$ up to $94.95 \pm 3.46\%$ is measured. Such high-spectral-purity photons will improve the visibility of quantum interference and facilitate the development of on-chip quantum information processing. Moreover, this concise and reconfigurable AMZI-coupled microring is a fabrication-friendly structure of a high-spectral-purity single-photon source. We can still get high-spectral-purity single photons by the configuration of AMZI, even if the bias exists in the fabrication of the AMZI-coupled microrings.

## Acknowledgments

Project supported by the National Basic Research Program of China (Grant Nos. 2019YFA0308700 and 2017YFA0303700) and the Open Funds from the State Key Laboratory of High Performance Computing of China (HPCL, National University of Defense Technology).

## References

[1] Bennett C H and Brassard G 2014 *Theoretical Computer Science* **560** 7
[2] Gisin N, Ribordy G, Tittel W and Zbinden H 2002 *Rev. Mod. Phys.* **74** 145
[3] Knill E, Laflamme R and Milburn G J 2001 *Nature* **409** 46
[4] Browne D E and Rudolph T 2005 *Phys. Rev. Lett.* **95** 010501
[5] Michler P, Kiraz A, Becher C, Schoenfeld W V, Petroff P M, Zhang L D, Hu E and Imamoglu A 2000 *Science* **290** 5500
[6] Santori C, Pelton M, Solomon G, Dale Y and Yamamoto Y 2001 *Phys. Rev. Lett.* **86** 1502
[7] Kuhn A, Hennrich M and Rempe G 2002 *Phys. Rev. Lett.* **89** 067901
[8] McKeever J, Boca A, Boozer A D, Miller R, Buck J R, Kuzmich A and Kimble H J 2004 *Science* **303** 1992
[9] Kurtsiefer C, Mayer S, Zarda P and Weinfurter H 2000 *Phys. Rev. Lett.* **85** 290

[10] Engin E, Bonneau D, Natarajan C M, Clark A S, Tanner M G, Hadfield R H, Dorenbos S N, Zwiller V, Ohira K, Suzuki N, Yoshida H, Iizuka N, Ezaki M, O'Brien J L and Thompson M G 2013 *Opt. Express* **21** 027826
[11] Spring J B, Mennea P L, Metcalf B J, Humphreys P C, Gates J C, Rogers H L, Söller C, Smith B J, Kolthammer W S, Smith P G R and Walmsley I A 2017 *Optica* **4** 90
[12] Lu X Y, Li Q, Westly D A, Moille G, Singh A, Anant V and Srinivasan K 2019 *Nat. Phys.* **15** 373
[13] Strain M J, Lacava C, Meriggi L, Cristiani I and Sorel M 2015 *Opt. Lett.* **40** 1274
[14] Bristow A D, Rotenberg N and van Driel H M 2007 *Appl. Phys. Lett.* **90** 191104
[15] Wu C, Liu Y W, Gu X W, Xue S C, Yu X X, Kong Y C, Qiang X G, Wu J J, Zhu Z H and Xu P 2019 *Chin. Phys. B* **28** 104211
[16] Wu C, Liu Y W, Gu X W, Yu X X, Kong Y C, Wang Y, Qiang X G, Wu J J, Zhu Z H, Yang X J and Xu P 2019 *Sci. China: Phys., Mech. Astron.* **63** 220362
[17] Vernon Z, Menotti M, Tison C C, Steidle J A, Fanto M L, Thomas P M, Preble S F, Smith A M, Alsing P M, Liscidini M and Sipe J E 2017 *Opt. Lett.* **42** 3638
[18] Liu Y W, Wu C, Gu X W, Kong Y C, Yu X X, Ge R Y, Cai X L, Qiang X G, Wu J J, Yang X J and Xu P 2017 *Opt. Lett.* **45** 73
[19] Zhu P Y, Liu Y W, Wu C, Xue S C, Yu X Y, Zheng Q L, Wang Y, Qiang X G, Wu J J and Xu P 2020 *Chin. Phys. B* **29** 114201
[20] Helt L G, Yang Z S, Liscidini M and Sipe J E 2010 *Opt. Lett.* **35** 3006
[21] Silverstone J W, Santagati R, Bonneau D, Strain M J, Sorel M, O'Brien J L and Thompson M G 2015 *Nat. Commun.* **6** 7948
[22] Dai Z, Liu Y, Xu P, Xu W X, Yang X J and Wu J J 2020 *Sci. China: Phys., Mech. Astron.* **63** 250311
[23] Gatti A, Corti T, Brambilla E and Horoshko D B 2012 *Phys. Rev. A* **86** 053803
[24] Liscidini M and Sipe J E 2013 *Phys. Rev. Lett.* **111** 193602